Laser spectroscopy of the $B0^+$ state in HgZn

J. Supronowicz, W. Kedzierski, J. B. Atkinson, and L. Krause
Department of Physics, University of Windsor, Windsor, Ontario, Canada N9B 3P4
and Ontario Laser and Lightwave Research Centre, Windsor, Ontario, Canada N9B 3P4
(Received 8 April 1991)

Excitation and fluorescence spectra of the HgZn excimer were observed in a mixture of Hg and Zn vapors contained in a quartz cell and subjected to pump-and-probe pulsed-laser excitation. The excitation spectrum extended from about 6600 Å to over 8000 Å; in the 6900–7700-Å region it exhibited some structure, but elsewhere it appeared to be structureless. The fluorescence spectrum was recorded in the 2600–2750-Å region and appeared as a series of Condon diffraction patterns arising from the bound-free decays of various vibronic states to the repulsive ground state. We believe the excitation spectrum to arise from $B0^+ \leftarrow A1$ vibronic transitions and the fluorescence spectrum from $B0^+ \rightarrow X0^+$ transitions.

PACS number(s): 33.20.−t, 33.50.Dq

We have been carrying out an extensive systematic study of laser-induced fluorescence (LIF) and excitation spectra of the HgZn excimer molecule [1–6], in the course of which we observed a weak excitation band in the 6400–7900-Å region, monitored on the 2751-Å fluorescence component [1]. We now report further experimental work on this band, which we identified in terms of vibronic transitions between spin-orbit states of the HgZn molecule [3].

The experiments were performed with apparatus quite similar to that described previously, using the pump and probe method [1,2,7]. Since the far-red dyes that were used in the probe laser are not very efficient when pumped by a N_2 laser, both pump and probe radiation were produced with the aid of the frequency-doubled output of a Q-switched Nd:YAG laser (where YAG denotes yttrium aluminum garnet). One part of the 5320-Å YAG beam was used to pump a dye laser whose output at 6152 Å was frequency doubled with a potassium dihydrogen phosphate C crystal to produce 8-ns pulses of 3076-Å radiation used to excite the $4\,^3P_1 \leftarrow 4\,^1S_0$ intercombination transition in Zn. The other part of the 5320-Å YAG radiation was used to pump a second (probe) dye laser which was operated with oxazine 725 and 750 dyes in methanol over a wavelength range 6600–8400 Å. As the process of producing LIF in the HgZn molecules requires a time delay between the pump and probe pulses [2], the probe-laser output was subsequently passed through a 50-m fiber that provided a delay of about 280 ns between the two pulses. The probe beam emerging from the fiber was collimated using a short-focal-length spherical lens and was weakly focused in the fluorescence cell, where it overlapped with the region illuminated by the (antiparallel) pump beam.

Excitation spectra were recorded by scanning the probe laser while monitoring the fluorescence intensity at a particular wavelength, and fluorescence spectra by scanning the monochromator across the fluorescence band with the probe laser set at a constant wavelength. The scanning increments were usually 1 Å for the excitation spectra and 2–4 Å for the fluorescence spectra.

Figures 1 and 2 show an excitation spectrum spanning the range 6850–7700 Å. The 7100–7200-Å gap in the spectrum is due to the lack of a suitable dye which could be used to produce sufficiently strong excitation. As may be seen, the spectrum has an intense continuous background with some structure in the 6900–7800-Å region. The continuum was found to extend from 6600 to 8300 Å, but outside these limits the signal rapidly decreased in intensity. Probe-laser irradiation at various wavelengths in this spectral region gave rise to fluorescence bands extending from 2600 to 2800 Å.

Figure 3 shows some typical fluorescence spectra that were excited with various probe-laser wavelengths. The spectra have similar intensity profiles; the most intense peak appears between 2730 and 2750 Å and several much

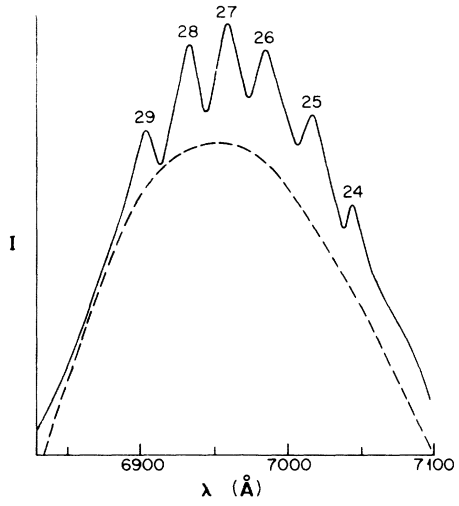

FIG. 1. A trace of the $B0^+ \leftarrow A1$ excitation spectrum in the 6830–7100-Å range, monitored at 2750 Å. The components of a $v' \leftarrow v''=0$ progression are tentatively identified. The dashed line represents the dye-laser power curve.

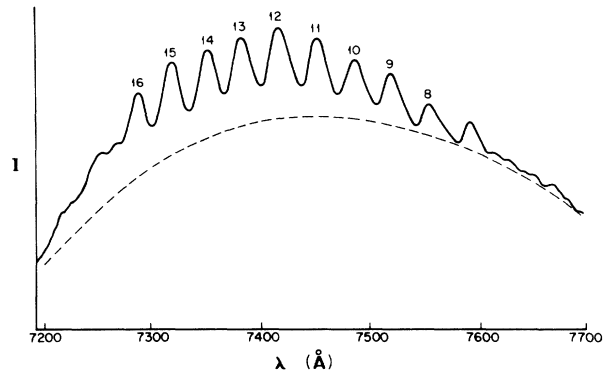

FIG. 2. A trace of the $B0^+ \leftarrow A1$ excitation spectrum in the 7200–7700-Å range, monitored at 2750 Å. See the caption for Fig. 1.

weaker components extend towards the short-wavelength wing of each spectrum, gradually diminishing and merging into the background. Similar intensity profiles were obtained using a variety of probe wavelengths in the range 6600–8000 Å. We believe that the spectra are due to the decay of bound excited vibronic states to the repulsive ground state, and represent fragments of Condon internal diffraction (CID) patterns [1,2]. The peak corresponding to the outer turning point of the vibrational wave function in the excited state, which normally appears at the short-wavelength end of each pattern, cannot

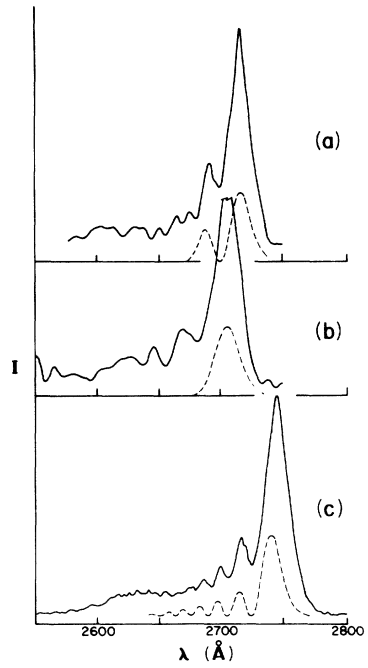

FIG. 3. Traces of bound-free fluorescence spectra, showing CID patterns. ——, experimental data; — — —, modeled spectrum. (a) 7860-Å excitation, $v'=1$, decay; (b) 7730-Å excitation, $v'=0$ decay; (c) 7560-Å excitation, most probably $v'=8$ decay.

be seen in the traces and the most prominent feature of the spectra is the peak corresponding to the inner turning point. This might be due to the fact that at the very high Hg vapor pressures in the cell (over 2.2 atm) there is significant absorption of light on the long-wavelength wing of the broadened 2537-Å Hg intercombination line, which can distort the shape of the spectra. We have noted a similar effect in $C0^+ \rightarrow X0^+$ fluorescence bands in HgZn [3,4]. Another factor that could contribute to the unusual profile of the Condon pattern would be a variation of the electronic transition moment with internuclear separation R, with a large moment at small R values rapidly decreasing towards larger internuclear separations. The rather low signal-to-noise ratio (SNR) in this spectrum makes unambiguous identification of the traces rather difficult. The peaks in the intensity profile of the excitation spectrum in Figs. 1 and 2 arise from the excitation of particular vibronic states, but the intense background continuum indicates that more than one vibrational level becomes excited at any particular wavelength setting of the probe laser.

The wavelength regions and intensity profiles of the excitation and fluorescence spectra shown in Figs. 1–3, considered in conjunction with the potential-energy (PE) diagram [3] and selection rules, permit an assignment of the spectra with a reasonable degree of confidence. We believe that the structure of the excitation spectrum shown in Figs. 1 and 2 represents a vibrational v' progression, since its spacing, of the order of 65–70 cm^{-1}, is much smaller than the vibrational spacing in the $A0^{\pm}$ and $A1$ reservoir states (~ 195 cm^{-1}) [3,4]. In spite of considerable efforts we did not succeed in observing a v'' progression in the excitation spectrum. The close spacing of v' components and their relative intensities suggest that the upper electronic state associated with the excitation spectrum has a rather shallow potential well with the equilibrium internuclear separation R_e considerably larger than in the reservoir states, since there appears to be little variation among the intensities of the vibrational components. These observations lead to the conclusions that the excitation spectrum arises from $B0^+ \leftarrow A1$ vibronic transitions and the fluorescence spectrum from the $B0^+ \rightarrow X0^+$ bound-free decays. The PE curves for several states [3] are shown in Fig. 4, where it may be seen that the $B0^+$ state has indeed the attributes inferred from the spectra. The energy separations (at the appropriate R values) between the $B0^+$, $A1$, and $X0^+$ curves are in good agreement with the recorded wavelengths of the spectra. It may also be seen in Fig. 4 that the $B0^+$ state, which has a triplet character, is perturbed at small internuclear separations by an avoided crossing with the singlet $C0^+$ state, where it exhibits a residual second well. The $C0^+$ state has a large probability of transition to the ground state, which manifests itself by the intense fluorescence spectrum in the 2400–2600-Å region [1–3]. On the other hand, the $B0^+$ state would be expected to have a much smaller probability for transitions to the ground state because of its triplet character. However, as the result of the avoided crossing, the $B0^+$ state undergoes a change of character near $R=R_x$ (where R_x is the internuclear separation at the avoided

crossing), becoming a singlet state at $R < R_x$ where it has a large transition probability for $B0^+ \rightarrow X0^+$ decay. At $R > R_x$ the state has a triplet character, accounting for the $B0^+ \leftarrow A1$ excitation spectrum. A similar effect has been observed in the spectrum of the Zn_2 excimer [8].

The PE curves are drawn on the basis of preliminary calculations [3] and their precise shapes are still subject to final adjustment. Accordingly, the exact location and extent of the avoided crossing should also be regarded as approximate, though there is no doubt as to its existence.

To test this interpretation, we carried out a computer-simulation of the bound-continuum spectra shown in Fig. 3. We have discussed the generation of the CID patterns in a previous article [9]. The intensity of the emitted fluorescence $I(E)$ may be represented as a function of the photon energy (E) [10]:

$$I(E) = \left[\int_0^\infty \psi_u(R) \psi_g((E_{v'} - E), R) dR \right]^2 , \quad (1)$$

where $E_{v'}$ is the total energy of the upper vibronic state and $E_{v'} - E$ is the total energy of the lower continuum state at which the transition terminates. Equation (1) neglects the rotational structure of the vibrational levels and the variation of the electronic transition moment with R. It also neglects the ν^3 dependence of the intensity, which is justified for a narrow spectral range [11]. In modeling Eq. (1) both upper and ground states were represented by Morse functions [12]. The potential well depth of the ground state was taken as the geometric mean of the corresponding Hg_2 and Zn_2 well depths [13]:

$$D_e(\text{HgZn}) = [D_e(\text{Hg}_2) D_e(\text{Zn}_2)]^{1/2} \sim 310 \text{ cm}^{-1} . \quad (2)$$

The vibrational frequency ω_e'' was chosen to make the shape of the ground-state PE curve conform to recent theoretical calculations [14] and was further adjusted during the modeling procedure. ω_e' was initially taken as 75 cm^{-1}, to correspond to the observed spacing of the v' progression in the excitation spectrum (which was corrected for anharmonicity). The upper-state vibronic wave functions ψ_u were analytical solutions of the Morse potential [12] and the continuum wave functions ψ_g of the ground state were generated using the JWKB method with Langer's condition [15], to obviate the singularities in the wave functions at the classical turnings points. The integrand in Eq. (1) was modified to incorporate variation of the transition moment with R, by taking

$$f(R) = b - aR , \quad (3)$$

and it was arbitrarily assumed that at $R = 5.67$ bohr (3 Å) the transition moment equaled 1. This rather crude approach, which was used in the absence of better theoretical estimates, produced the most reasonable results when the transition moment at $R = 3$ Å was about ten times larger than at $R = 4$ Å (7.56 bohr).

The modeled profiles of the fluorescence spectra are drawn in Fig. 3 in juxtaposition with the profiles recorded experimentally. The fit between the two sets of spectra is only moderately good, as might be expected in view of the various assumptions made in the modeling calculations, to which reference was made above. The assumption that each fluorescence spectrum is due to the decay of a single vibronic state is only partly correct. The difference $R_e' - R_e''$ between the equilibrium internuclear separations of the $B0^+$ and $A1$ states is rather large, which causes the broadening of the $A1$ vibrational components in excitation, due to rotational structure; the broadening is further enhanced at the relatively high ambient temperature (840 K). The vibrational spacing in the $B0^+$ state is also much smaller than in the other excited HgZn states [1–6], which may cause some overlap of $B0^+$ rovibrational levels as well as their collisional mixing. Accordingly, we believe that each of the fluorescence spectra in Fig. 3 arises predominantly (but not exclusively) from the decay of a particular vibronic state. This conclusion is supported by the profiles of the excitation spectrum shown in Figs. 1 and 2 which show structure together with a high continuum background level, and of further unstructured segments of this spectrum, which are not shown here. Assuming [as is done in Fig. 3(c)] that 7560-Å probe radiation excited the $v' = 8$ vibrational level of the $B0^+$ state, an attempt could be made to identify the vibrational components in the excitation spectrum. The regular progression which may be seen in Fig. 2 suggests that the excitation is effected from a single $A1$ vibrational level, possibly the $v'' = 0$ level. We have attempted a tentative assignment of the vibrational v' progression, which includes a component at 7560 Å, as shown in Figs. 2 and 3. The correctness of the assignment relies on the identification of the component at 7560 Å as due to $v' = 8$, which we estimate as being accurate within ± 2 vibrational quantum numbers. The molecular constants for the $X0^+$ and $B0^+$ states, which were yielded by the modeling process, are listed in Table I.

We should make a brief comment on the origin of the continuum in the excitation spectrum, which is apparent in Figs. 1 and 2 and extends beyond the wavelength limits of the traces. An excitation spectrum monitored on a bound-free fluorescence band is usually less structured than when monitored on a component of a bound-bound spectrum. This unstructured quality is enhanced when the difference $R_e' - R_e''$ is large and the vibrational spacing ω_e of one of the participating states is small. A large $R_e' - R_e''$ corresponds to a large difference between the rotational constants $B_{v'} - B_{v''}$ and causes a large range of rotational levels (and frequencies) to participate in the excitation process and to give rise to the broadband emission detected by the monochromator, causing the "washing out" of the band structure without diminishing the signal. When the upper state has a small vibrational

TABLE I. Molecular constants for the $X0^+$ and $B0^+$ states of HgZn.

Designation	$X0^+$	$B0^+$
R_e (Å)	4.66	3.66
ω_e (cm^{-1})	19.3	72.0
$\omega_e x_e$ (cm^{-1})	0.3	0.4
T_e (cm^{-1})[a]	−310	37 360

[a]Relative to the energy of two separated ground-state atoms.

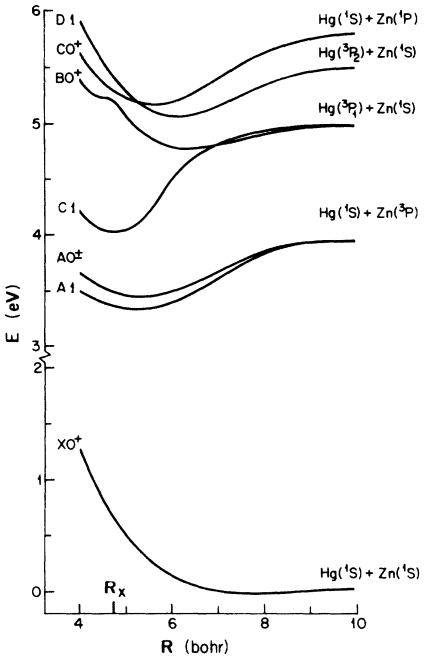

FIG. 4. A partial PE diagram showing the states involved in the excitation and decay processes. The PE curves were taken from Ref. [3].

spacing, this causes overlap between the vibrational bands increasing the signal density within the detection bandwidth and causing the signal modulation with the wavelength to be partly submerged in the background. Both conditions apply in the present case, creating a situation similar to that observed in the $C0^+ \leftarrow A0^+$ band of HgZn [3] and the $G0_u^+ \leftarrow A0_g^+$ band of Hg_2 [16].

We understand that the Morse potential can be safely used to represent only the attractive part of the $X0^+$ ground state but to a lesser extent the $B0^+$ state which is perturbed and whose vibrational structure, although quite evident over a 1100-cm^{-1} range, cannot therefore be extrapolated towards lower v' values. The assumption of the Morse potential for the repulsive part of the ground state (which plays a crucial role in the formation of CID spectra) is also an approximation. The experimental situation was further complicated by the relative location of the PE curves. In the probe-wavelength region where the excitation spectrum has a regular structure, the resulting fluorescence spectra originated from high v' states, making difficult the unambiguous identification of the v' level. On the other hand, the probe wavelengths that produced clear fluorescence spectra, originating from low v' levels, lay in a wavelength region in which the excitation spectrum had an irregular and faint structure.

As may be seen in Fig. 4, the $B0^+$ PE curve has a relatively shallow well, as confirmed by the small ω_e' and well-depth values derived from the experiment and from the modeling calculations, which therefore confirm the *ab initio* theoretical calculations [3,14] that gave rise to the PE diagram.

This research was supported by the Canadian Department of National Defense, and by the Natural Sciences and Engineering Research Council of Canada.

[1] J. Supronowicz, E. Hegazi, G. Chambaud, J. B. Atkinson, W. E. Baylis, and L. Krause, Phys. Rev. A **37**, 295 (1988).
[2] J. Supronowicz, E. Hegazi, J. B. Atkinson, and L. Krause, Phys. Rev. A **37**, 3818 (1988); **39**, 4892 (1989).
[3] E. Hegazi, J. Supronowicz, G. Chambaud, J. B. Atkinson, W. E. Baylis, and L. Krause, Phys. Rev. A **40**, 6293 (1989).
[4] E. Hegazi, J. Supronowicz, J. B. Atkinson, and L. Krause, Phys. Rev. A **42**, 2734 (1990).
[5] E. Hegazi, J. Supronowicz, J. B. Atkinson, and L. Krause, Phys. Rev. A **42**, 2741 (1990).
[6] E. Hegazi, J. Supronowicz, J. B. Atkinson, and L. Krause, Phys. Rev. A **42**, 2745 (1990).
[7] J. Niefer, J. Supronowicz, J. B. Atkinson, and L. Krause, Phys. Rev. A **34**, 1137 (1986).
[8] W. Kedzierski, J. Supronowicz, J. B. Atkinson, W. E. Baylis, L. Krause, M. Couty, and G. Chambaud, Chem. Phys. Lett. **175**, 221 (1990).
[9] R. J. Niefer, J. Supronowicz, J. B. Atkinson, and L. Krause, Phys. Rev. A **34**, 1137 (1986).
[10] R. S. Mulliken, J. Chem. Phys. **55**, 309 (1971).
[11] D. Eisel, D. Zevgolis, and W. Demtröder, J. Chem. Phys. **71**, 2005 (1979).
[12] P. M. Morse, Phys. Rev. **34**, 57 (1929).
[13] H. Kuhn and S. Arrhenius, Z. Phys. **82**, 716 (1933); J. O. Hirschfelder, C. F. Curtiss, and R. B. Bird, *Molecular Theory of Gases and Liquids* (Wiley, New York, 1954); M. Czajkowski, R. Bobkowski, and L. Krause, Phys. Rev. A **41**, 277 (1990).
[14] J. Sienkiewicz and W. E. Baylis (private communication).
[15] P. E. Langer, Phys. Rev. **51**, 669 (1937).
[16] J. Supronowicz, R. J. Niefer, J. B. Atkinson, and L. Krause, J. Phys. B **19**, 1153 (1986); **19**, L717 (1986).